A Combined Experimental and Theoretical Study on the Formation of Interstellar C3H Isomers

R. I. Kaiser; C. Ochsenfeld; M. Head-Gordon; Y. T. Lee; A. G. Suits

Science is currently published by American Association for the Advancement of Science.

the influences of temperature and salinity changes in the Sargasso Sea surface are additive, whereas they tend to cancel each other at other locations.

24. D. R. Cayan, *J. Clim.* **5**, 354 (1992); Y. Kushnir, *ibid.* **7**, 141 (1994).
25. R. R. Dickson and J. Namias, *Mon. Weather Rev.* **104**, 1255 (1976).
26. Equilibrium calcite precipitation was calculated using annual average Station "S" data, the North Atlantic salinity-$\delta^{18}O$ relationship [H. Craig and L. I. Gordon, *Symposium on Marine Geochemistry (Occas. Publ. 3*, Narragansett Marine Laboratory, Naragansett, RI, 1965)], and Shackleton's paleotemperature equation [N. J. Shackleton, *CNRS Colloq.* **219**, 203 (1974)].
27. Using the calibration of M. Stuiver and P. J. Reimer, *Radiocarbon* **35**, 215 (1993).
28. Subcores A and D were analyzed on two different mass spectrometers (a VG Prism and a partially automated VG Micromass 903, respectively). Although there might be a slight intercalibration difference be-

tween the two instruments, the small differences among the $\delta^{18}O$ results most likely reflect sedimentary processes such as bioturbation. All data are archived at the NOAA/NGDC World Data Center-A for Paleoclimatology (paleo@mail.ngdc.noaa.gov).

29. R. S. Bradley and P. D. Jones, *Holocene* **3**, 367 (1993).
30. J. Patzold and G. Wefer, paper presented at the *Fourth International Conference on Paleoceanography*, Kiel, p. 224 (1992); R. B. Dunbar and J. E. Cole, *Coral Records of Ocean-Atmosphere Variability* (University Corporation for Atmospheric Research, Boulder, CO, 1993).
31. E. M. Druffel, *Science* **218**, 13 (1982).
32. C. K. Folland, T. N. Palmer, D. E. Parker, *Nature* **320**, 602 (1986).
33. M. R. Talbot and G. Delibrias, *ibid.* **268**, 722 (1977); *Earth Planet. Sci. Lett.* **47**, 336 (1980).
34. K. R. Briffa *et al.*, *Nature* **346**, 434 (1990); *Clim. Dynam.* **7**, 111 (1992).

35. J. A. Matthews, *Holocene* **1**, 219 (1991).
36. J. M. Mitchell Jr., *Quat. Res.* **6**, 481 (1976).
37. J. E. Kutzbach and R. A. Bryson, *J. Atmos. Sci.* **31**, 1958 (1974).
38. S. J. Lehman and L. D. Keigwin, *Nature* **358**, 198 (1992).
39. D. W. Oppo and S. J. Lehman, *Science* **259**, 1148 (1993).

A Combined Experimental and Theoretical Study on the Formation of Interstellar C₃H Isomers

R. I. Kaiser, C. Ochsenfeld, M. Head-Gordon, Y. T. Lee, A. G. Suits

The reaction of ground-state carbon atoms with acetylene was studied under single-collision conditions in crossed beam experiments to investigate the chemical dynamics of forming cyclic and linear C₃H isomers (c-C₃H and l-C₃H, respectively) in interstellar environments via an atom-neutral reaction. Combined state-of-the-art ab initio calculations and experimental identification of the carbon-hydrogen exchange channel to both isomers classify this reaction as an important alternative to ion-molecule encounters to synthesize C₃H radicals in the interstellar medium. These findings strongly correlate with astronomical observations and explain a higher [c-C₃H]/[l-C₃H] ratio in the dark cloud TMC-1 than in the carbon star IRC+10216.

For more than two decades, networks of radiative association, dissociative recombination, and exothermic ion-molecule reactions have been postulated to account for chemistry in the interstellar medium (ISM) (*1*). Such reactions involve ubiquitous radicals such as linear and cyclic C₃H (*l*-C₃H, propynylidyne, and *c*-C₃H, cyclopropynylidene) (*2*); for example, addition of C⁺ to C₂H₂ yielding *l/c*-C₃H⁺ + H is thought to be followed by a subsequent radiative association of *l/c*-C₃H⁺ and H₂ to *c*-C₃H₃⁺, and a final dissociative electron-ion recombination forming *l/c*-C₃H and two hydrogen atoms or H₂. This framework, however, cannot reproduce observed number densities and isomer ratios. Fueled by recent kinetic studies of barrierless, fast neutral-neutral reactions of atomic carbon C(^3P_j) with unsaturated hydrocarbons (*3*), Herbst and co-workers implemented this reaction class into generic models of the dark molecular cloud

Department of Chemistry, University of California, Berkeley, CA 94720, USA, and Chemical Sciences Division, Lawrence Berkeley National Laboratory, Berkeley, CA 94720, USA.

TMC-1 and the circumstellar envelope surrounding the carbon star IRC+10216 to improve the fit to astronomical surveys (*4*). These models, however, suffer from sparse laboratory data on reaction products and cannot elucidate the contribution to distinct structural isomers such as *l/c*-C₃H. Therefore, even this refined network does not explain the interstellar *c*-C₃H to *l*-C₃H ratio of unity in cold molecular clouds compared to 0.2 ± 0.1 around IRC+10216. Hence the formation of interstellar C₃H isomers remains to be resolved.

In this report, we present combined high-level ab initio calculations and crossed-beam experiments on the atom-neutral reaction 1 to interstellar C₃H isomers via C₃H₂ intermediates:

$$C(^3P_j) + C_2H_2(X^1\Sigma_g^+) \rightarrow C_3H_2 \rightarrow$$

$$l\text{-}C_3H(X^2\textstyle\prod_j) + H(^2S_{1/2}) \qquad (1a)$$

$$c\text{-}C_3H(X^2B_2) + H(^2S_{1/2}) \qquad (1b)$$
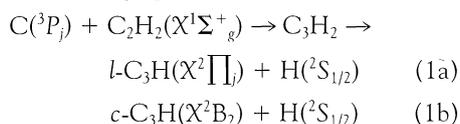
This system represents the prototype reaction of ubiquitous interstellar carbon atoms with the simplest unsaturated hydrocarbon

molecule, acetylene, to synthesize hydrocarbon radicals via a single atom-neutral collision in interstellar environments. The circumstellar shell of IRC+10216, for example, contains C₂H₂ as well as C(^3P_j) reservoirs at distances of 10^{14} to 10^{15} m from the central star (*5*), and formation of C₃H via reaction 1 is feasible. Our investigations also provide dynamical information on the elementary steps to C₃H isomers. The laboratory data strongly depend on the structures of the initially formed C₃H₂ collision complexes, and therefore we first calculated the ab initio geometries of energetically accessible C₃H₂ isomers. We then compared our crossed-beam data and experimental dynamics with those arising from distinct C₃H₂ adducts. Once the isomers were identified, we determined the exit channels from C₃H₂ following a carbon-hydrogen bond rupture to *c*-C₃H, or *l*-C₃H, or both.

Ab initio electronic structure calculations were performed at a level of theory high enough to predict relative energies of all local minima and reaction exothermicities to a precision of about 1 to 3 kJ mol⁻¹ (*6*). The discussion is limited to the triplet potential energy surface (PES) because no triplet C₃H₂ minimum fulfills the requirements for intersystem crossing (*7*). Our ab initio calculations show that propargylene, HCCCH, is the global minimum on the triplet C₃H₂ PES and is bound by 385.4 kJ mol⁻¹ with respect to the reactants (Fig. 1 and Table 1). The structure has an almost linear C–C–C angle of 171.9° and a torsion angle between the two hydrogen bonds of 88.0°. Its C₂ symmetry agrees with recent experimental Fourier transform infrared spectroscopy assignments based on isotope substitution studies in argon matrices (*8*). A second isomer, vinylidenecarbene, H₂CCC, has C₂ᵥ symmetry and lies 134.9 kJ mol⁻¹ above propargylene. Its enthalpy of formation ΔH_f° (0 K) = 678.6 kJ mol⁻¹ is in excellent agreement with an experimen-

tally determined value of 668 ± 30 kJ mol^{-1} (9). Triplet cyclopropenylidene, c-C_3H_2, is situated 172.4 kJ mol^{-1} above propargylene and shows no symmetry element. One hydrogen is placed almost in the plane of the carbon tricycle, whereas the second H atom is distorted out of the CCC plane. Another isomer, s-$trans$-propenediylidene, CCHCH, (C_s symmetry) lies an additional 78.4 kJ mol^{-1} higher in energy. The most stable isomer on the doublet C_3H PES is a cyclic structure with C_{2v} symmetry (10). A linear geometry ($C_{\infty v}$) and a slightly distorted linear structure (C_s) (C–C–C bond angle of 174.0°; H–C–C bond angle of 156.5°) are virtually isoenergetic. The lowest vibrational frequency of C_3H of only 208 cm^{-1} indicates the extreme floppiness of the bent isomer. Both structures are ~7 kJ mol^{-1} higher in energy than the cyclic one. Our calculations give a reaction exothermicity of 1.5 kJ mol^{-1} for the overall reaction 1a to form l-$C_3H(X^2\Pi_i)$ + $H(^2S_{1/2})$, and of 8.6 kJ mol^{-1} for (1b) to yield c-$C_3H(X^2B_2)$ + $H(^2S_{1/2})$.

The experiments were performed under single-collision conditions at three different collision energies (8.8, 28.0, and 45.0 kJ mol^{-1}) with a universal crossed molecular beam apparatus (11). The 266-nm output of a Nd:yttrium-aluminum-garnet (YAG) laser was focused on a rotating carbon rod, and ablated C atoms were seeded into Ne or He carrier gas (12). The carbon beam crossed a continuous acetylene beam at 90° in the interaction region, and time-of-flight (TOF) spectra and product angular distributions in the laboratory frame of reactively scattered products were monitored with a quadrupole mass spectrometer with an electron-impact ionizer. Information on the reaction dynamics was obtained by fitting our data with a forward-convolution routine (13), which yielded the angular flux distribution $T(\theta)$ and the translational-energy flux distribution $P(E)$ in the center-of-mass system.

In the laboratory angular distributions and TOF spectra (see Figs. 2 and 3 for data at a selected collision energy), no radiative association to C_3H_2 was detected. The identification of this C-H exchange under single-collision conditions alone underlines the potential importance of this reaction to build up C_3H radicals in interstellar environments. In addition, this result demonstrates that the highly internally excited C_3H_2 adduct does not survive under the single-collision conditions in our experiments and in the interstellar medium; however, denser planetary or cometary atmospheres can supply a third-body reaction to stabilize the reac-

tion intermediate.

The crossed-beam method and ab initio studies provide further insight into the chemical dynamics of the reaction and reveal information on reaction intermediates as well as C_3H isomers. The $P(E)$ and $T(\theta)$ of reaction 1 were inferred from the experimental results (Fig. 4). All $P(E)$s peak between 5 and 10 kJ mol^{-1}, suggesting an almost barrierless bond-rupture process via a loose exit-transition state from the decomposing C_3H_2 reaction intermediate to the products. The high energy cutoffs of the $P(E)$s are in excellent agreement with our ab initio reaction exothermicities plus the relative collision energy. The discrepancies of about 4 to 7 kJ mol^{-1} fall within the error limits of the peak collision energies and the accuracy of the ab initio calculations. Our calculations in-

dicate that c-C_3H is more stable by 7 kJ mol^{-1} than l-C_3H; therefore the possible isomers cannot be assigned based solely on the $P(E)$s, and the center-of-mass $T(\theta)$s must be analyzed in detail.

With increasing collision energy, the form of the center-of-mass $T(\theta)$s (Fig. 4) changes significantly. A decreasing for-
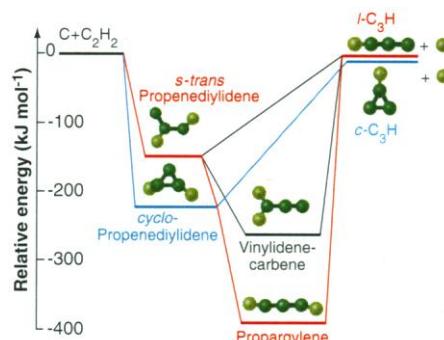
Fig. 1. Calculated ab initio structures and relative energies of triplet C_3H_2 and doublet C_3H isomers; dark green balls denote carbon atoms, light green balls hydrogen atoms. Proposed reaction pathways have been inferred from our crossed beam experiments, as discussed in the text. Blue lines denote our proposed reaction pathway to the c-C_3H isomer, the red lines to l-C_3H. Black lines depict pathways not involved in the present reaction.
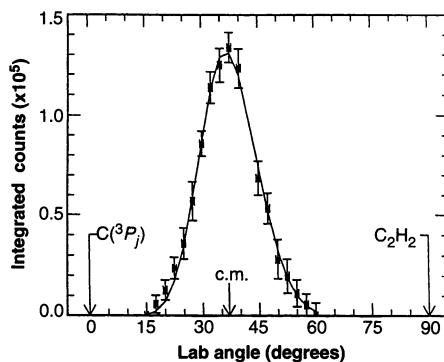
Fig. 2. Laboratory angular distribution of C_3H at mass to charge ratio m/e = 37 at a collision energy of 28.0 kJ mol^{-1}. Circles and 1σ error bars indicate experimental data, the solid lines the calculated distribution, and c.m. the center-of-mass angle.

Fig. 3. Time-of-flight data at m/e = 37 at a collision energy of 28.0 kJ mol^{-1}. Open circles represent experimental data, the solid line the fit. The TOF spectra were normalized to the relative intensity at each angle.
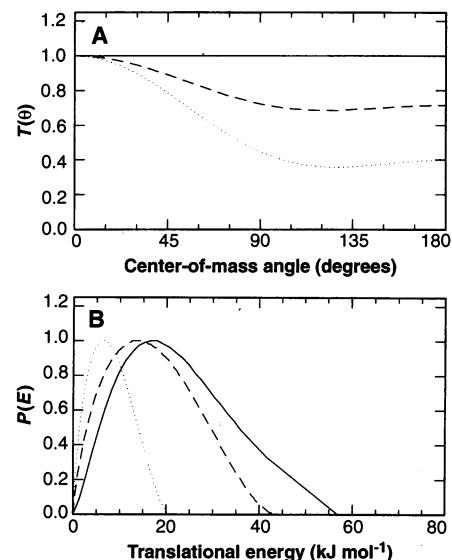
Fig. 4. The center-of-mass (A) angular and (B) translational energy flux distributions for the reaction $C(^3P_j)$ + $C_2H_2(X^1\Sigma_g^+)$ at peak collision energies of 8.8 (dotted line), 28.0 (dashed line), and 45.0 kJ mol^{-1} (solid line).

ward-backward intensity ratio at the poles from 2.6 (8.8 kJ mol^{-1}) through 1.2 (28.0 kJ mol^{-1}) to 1.0 (45.0 kJ mol^{-1}) is observed, resulting from the disappearance of forward-peaked products with respect to the carbon beam at higher collision energy and suggesting that each $T(\theta)$ can be decomposed into two distinct micromechanisms. The first microchannel involves a flat, forward-backward symmetric $T(\theta)$, independent of the collision energy. This can be attributed either to a C_3H_2 collision complex with a lifetime longer than its rotational period or to a symmetric reaction intermediate in which both H atoms can be interconverted by a rotation around a principal axis and hence depart with equal probability into the center-of-mass angles θ and π-θ (14). The second microchannel shows a strong forward peaking with respect to the carbon beam. This contribution is quenched as the collision energy rises. By integrating the

product of the center-of-mass distributions, $T(\theta)*P(E)$, we obtain a relative cross-section ratio of [σ(8.8 kJ mol^{-1})/ σ(28.0 kJ mol^{-1})] = 3.5 ± 1.4. This finding correlates qualitatively with bulk experiments (3) and shows that the reaction proceeds without entrance barrier. The deviation of our experimental ratio from the theoretical prediction of 1.3 calculated within the capture theory (15) indicates that the structure of the acetylene molecule plays a significant role when the orbiting radii fall below the van der Waals dimension of the C_2H_2 molecule.

We now attempt to resolve the chemical dynamics of the isotropic microchannel. An interpretation of a long-lived C_3H_2 collision complex contributing to an isotropic $T(\theta)$ can be dismissed. From the potential energy well depth of all C_3H_2 isomers relative to the reactants and products, propargylene is expected to have the longest lifetime at the collision energy of 45 kJ mol^{-1}. Even with a well depth of 385.4 kJ mol^{-1}, the lifetime of the reaction intermediate is expected to be less than the rotational period of the reaction intermediate. Comparing the dynamics with those of the reaction $C(^3P_j)$ + CH_3CCH (X^1A_1) (16) provides further support for this argument. In this study (16), the fragmenting methylpropargylene was shown to have a lifetime equivalent to its rotational period at a collision energy of 33.2 kJ mol^{-1} and, by analogy, a HCCCH complex with a lifetime less than its rotational period is expected because of the reduced number of nine vibrational modes in propargylene, compared to 18 in methylpropargylene. Microchannel one thus originates from a symmetric reaction intermediate, in which the two H atoms can be interconverted through a rotation. This restricts possible C_3H_2 complexes to H_2CCC or HCCCH. Based on our ab initio geometries, c-C_3H_2 and CCHCH have no symmetry axis and can be excluded. If H_2CCC were formed, the fragmenting complex would rotate around the C_2 axis to yield l-$C_3H(X^2\Pi_j)$ after C-H bond cleavage. The linear isomer would be excited to rotations around its internuclear axis, but because of the vanishing moment of inertia, this rotation is not energetically accessible, and this pathway cannot account for rotational excitation in l-C_3H. Although the slightly bent C_3H structure is a local minimum, this isomer behaves like a quasilinear molecule (17) because its bending mode can be easily excited. These arguments indicate that microchannel one very likely involves the HCCCH isomer rotating around its C_2 axis, leading to l-C_3H after a C-H bond rupture.

During the dynamic processes leading to the formation of HCCCH itself, direct insertion of $C(^3P_j)$ into the acetylenic C-H bond can be ruled out, because this symmetry-forbidden pathway is expected to involve a significant entrance barrier, much greater than our lowest collision energy of 8.8 kJ mol^{-1}. Further, an analogous reaction of $C(^3P_j)$ with methylacetylene exhibits no evidence of insertion into the acetylenic C-H bond (16). Therefore, HCCCH is very likely formed by an initial addition of a C atom to HCCH to yield CCHCH and a subsequent 2,3-H-migration. This pathway accounts for large reactive impact parameters close to the orbiting limit, as found experimentally. Further, the loose exit transition state of the final C-H bond rupture to l-$C_3H(X^2\Pi_j)$ and $H(^2S_{1/2})$ involves only minor geometry changes from the decomposing HCCCH to l-C_3H: C-C and C-H distances change by <0.07 Å, and the bending angle of the three propargylene C atoms opens by only 8.1° (Table 1).

The second, forward-scattered microchannel follows direct reaction dynamics. Large impact parameters and reaction intermediates with shallow potential energy wells contribute to the reactive scattering signal. Therefore, $C(^3P_j)$ insertion to form HCCCH can be excluded. The large deviation of the relative cross sections from classical capture theory (15) explains the underlying dynamics for this microchannel. Although the detailed structure of the molecule does not play a role within the simple capture framework, this approximation breaks down as the orbiting radius decreases with rising collision energy: Reactive encounters from radii exceeding the symmetric π-cloud to form c-C_3H_2 become more and more unlikely. Rather, they preferentially involve orbits in which the π-cloud can be attacked sideways to yield the CCHCH isomer. This model can explain both the decreasing cross section and the less polarized center-of-mass $T(\theta)$ as the collision energy is increased. The final C-H bond rupture would then form the c-C_3H isomer and an H atom.

Our crossed-beam studies combined with the presented ab initio calculations identify both isomers, the l-C_3H and c-C_3H, under single-collision conditions. This reaction represents a one-step encounter to build up C_3H isomers in the ISM and eliminates the need for successive binary encounters as required in ion-molecule networks. The proposed chemical dynamics that cause an increasing ratio of l-C_3H to c-C_3H with increasing collision energy can explain previously unresolved astronomical observations. Dark

Table 1. Structural data of C_3H_2 and C_3H isomers as depicted in Fig. 1. For structures with a C_2-symmetry axis (and not all C atoms situated on this axis, as in the H_2CCC structure, Fig. 1), the symmetry-unique C atom is labeled C*. C' is the symmetry equivalent of C. If no such symmetry exists, C and H atoms, respectively, are numbered from left to the right in Fig. 1 (for the cyclic isomer c-C_3H_2, the atom C-2 has no H atoms). H1-C2-C3-C1 stands for the out-of-plane angle between the bond H1-C1 and the plane C2C3C1, and H-C'-C-H' is a torsion angle.

Bond lengths (A)		Bond angles (degrees)	
		HCCCH	
C*-C	1.279	C-C*-C'	171.9
C-H	1.067	C*-C-H	156.5
		H-C'-C-H'	88.0
		H$_2$CCC	
C1-C2	1.369	H-C1-C2	120.5
C2-C3	1.238		
C1-H	1.081		
		c-C$_3$H$_2$	
C1-C2	1.448	H1-C1-C3	125.9
C2-C3	1.304	H2-C3-C1	141.4
C1-C3	1.551	H1-C2-C3-C1	46.1
C1-H1	1.088	H2-C1-C2-C3	0.2
C3-H2	1.073		
		CHCCH	
C1-C2	1.349	C1-C2-C3	121.2
C2-C3	1.392	C1-C2-H1	117.1
C2-H1	1.092	C2-C3-H2	134.1
C3-H2	1.079		
		c-C$_3$H	
C-C*	1.377		
C-C'	1.378		
C*-H	1.078		
		l-C$_3$H	
H-C1	1.065		
C1-C2	1.243		
C2-C3	1.347		
		b-C$_3$H	
H-C1	1.072	H-C1-C2	156.5
C1-C2	1.253	C1-C2-C3	174.0
C2-C3	1.336		

molecular clouds hold typical averaged translational temperatures of 10 K, whereas circumstellar shells around carbon stars are heated up to ~4000 K, giving mean translational energies of about 0.1 and 40 kJ mol^{-1}, respectively. Therefore, comparable amounts of both isomers are anticipated to be produced in dark clouds, whereas less c-C_3H than l-C_3H should be formed in the hotter envelope surrounding carbon stars such as IRC+10216. This expected pattern is reflected in the observed number density ratios of c-C_3H versus l-C_3H. Therefore a common HCCH reactant for the formation of interstellar l/c-C_3H radicals via atom-neutral reaction with C(^3P_j) must be included into interstellar reaction networks, taking account of distinct structural isomers.

This work is a step toward a better understanding of reactions of neutral atoms with neutral reactants in the interstellar medium. The direct observation of the C-H exchange channel represents a versatile synthetic route to reactive hydrocarbon radicals in the ISM. Interstellar environments of unsaturated hydrocarbons such as methylacetylene (CH_3CCH), ethinyl (C_2H), vinyl (C_2H_3), ethylene (C_2H_4), and propylene (C_3H_6) which overlap with large concentrations of atomic carbon should be sought. Once these regions have been charted, the search for hitherto unobserved interstellar radicals as reaction products of these atom-neutral reactions is open.

REFERENCES AND NOTES

1. E. Herbst and W. Klemperer, Astrophys. J. 185, 505 (1973); E. Herbst and J. Delos, Chem. Phys. Lett. 42, 54 (1976); E. Herbst, N. G. Adams, D. Smith, Astrophys. J. 285, 618 (1984); G. Winnewisser and E. Herbst, Top. Curr. Chem. (Springer, Berlin, 1987), p. 121; D. Smith, Chem. Rev. 92, 1580 (1992).
2. R. I. Kaiser, Y. T. Lee, A. G. Suits, J. Chem. Phys. 103, 10395 (1995).
3. D. C. Clary, N. Haider, D. Husain, M. Kabir, Astrophys. J. 422, 416 (1994).
4. T. J. Millar and E. Herbst, Astron. Astrophys. 288, 561 (1994); E. Herbst and C. M. Leung, Astrophys. J. 233, 170 (1990); D. C. Clary, T. S. Stoecklin, A. G. Wickham, J. Chem. Soc. Faraday Trans. 89, 2185 (1993); E. Herbst, H. H. Lee, D. A. Howe, T. J. Millar, Mon. Not. R. Astron. Soc. 268, 335 (1994); R. P. A. Bettens, H. H. Lee, E. Herbst, Astrophys. J. 443, 664 (1995); Q. Liao and E. Herbst, ibid. 444, 694 (1995).
5. J. Keene, K. Young, T. G. Phillips, T. H. Büttgenbach, Astrophys. J. 415, L131 (1993).
6. Our calculations used the CCSD(T) (single- and double-excitation coupled cluster with a perturbational estimate of triple excitations) level [K. Raghavachari, G. W. Trucks, J. A. Pople, M. Head-Gordon, Chem. Phys. Lett. 157, 479 (1989)] based on unrestricted Hartree-Fock (UHF) wave functions. Only the pure spherical harmonic components of d, f, and g functions were included. The ACES II program package was used [J. F. Stanton, J. Gauss, J. D. Watts, W. J. Lauderdale, R. J. Bartlett, Int. J. Quantum Symp. 26, 879 (1992)]. Structures of local minima were fully optimized using a triple zeta polarization (TZP) basis set [A. Schäfer, H. Horn, R. Ahlrichs, J. Chem. Phys. 97, 2571 (1992)], and stationary points were characterized by vibrational frequencies within the harmonic approximation. Vibrational frequencies were computed numerically with analytical CCSD(T) gradients [J. D. Watts, J. Gauss, R. J. Bartlett, Chem. Phys. Lett. 200, 1 (1992)]. Energy differences and reaction energies were obtained by single-point calculations with a quadruple zeta double polarization [QZ2P; H:(7s2p1d)/[4s2p1d]; C: (11s7p2d1f)/[6s4p2d1f]); A. Schäfer, H. Horn, R. Ahlrichs, J. Chem. Phys. 97, 2571 (1992)] and a correlation consistent polarized valence quadruple zeta [cc-pVQZ; H:(6s3p2d1f)/[4s3p2d1f]; C:(12s6p3d2f1g)/[5s4p3d2f1g] (T. H. Dunning, J. Chem. Phys. 90, 1007 (1989)] basis. Zero-point energies were included as computed at the CCSD(T)/TZP level; the zero-point vibrational energy of c-C_3H was taken from J. F. Stanton [Chem. Phys. Lett. 237, 20 (1995)].
7. N. J. Turro, Modern Molecular Photochemistry (University Science Books, Mill Valley, CA, 1991).
8. R. A. Seburg and R. J. McMahon, Angew. Chem. Int. Ed. Engl. 107, 2198 (1995).
9. M. S. Robinson, M. L. Polak, V. M. Bierbaum, C. H. DePuy, W. C. Lineberger, J. Am. Chem. Soc. 117, 6766 (1995).
10. J. F. Stanton, Chem. Phys. Lett. 237, 20 (1995).
11. Y. T. Lee, J. D. McDonald, P. R. LeBreton, D. R. Herschbach, Rev. Sci. Instrum. 40, 1402 (1969); Y. T. Lee, Science 236, 793 (1987). The peak velocities of the carbon beam were determined to 1180, 2463, and 3196 ms^{-1} and those of the acetylene beam to 866 ms^{-1}.
12. R. I. Kaiser and A. G. Suits, Rev. Sci. Instrum. 66, 5405 (1995).
13. E. A. Entenmann, thesis, Harvard University (1986).
14. W. B. Miller, S. A. Safron, D. R. Herschbach, Discuss. Faraday Soc. 44, 108, 291 (1967).
15. In this framework, the C atom orbits the HCCH molecule prior to reaction. The HCCH molecules are treated as point masses, and therefore sterical effects do not play a role in this simple model [R. D. Levine and R. B. Bernstein, Molecular Reaction Dynamics and Chemical Reactivity (Oxford Univ. Press, Oxford, 1987)]. Therefore, any deviation from this theory indicates that the actual structure of the HCCH molecule plays a significant role.
16. R. I. Kaiser, D. Stranges, Y. T. Lee, A. G. Suits, J. Chem. Phys., 105, 8705 (1996).
17. M. Kanada, S. Yamamoto, S. Saito, Y. Osamura, ibid. 104, 2192 (1996).
18. R.I.K. and C.O. are indebted to the Deutsche Forschungsgemeinschaft (DFG) for post-doctoral fellowships. C.O. thanks Prof. Jürgen Gauss, University of Mainz, Germany, and Dr. Dage Sundholm, University of Helsinki, Finland, for assistance in using the ACES II program system and providing a DEC version of this package. We gratefully acknowledge useful comments in reading this manuscript from J. Gauss (University of Mainz, Germany) and P. Casavecchia (University of Perugia, Italy). This work was supported by the Director, Office of Energy Research, Office of Basic Energy Sciences, Chemical Sciences Division of the U.S. Department of Energy under contract DE-AC03-76SF00098.

Essential Yeast Protein with Unexpected Similarity to Subunits of Mammalian Cleavage and Polyadenylation Specificity Factor (CPSF)

Guillaume Chanfreau,* Suzanne M. Noble,* Christine Guthrie†

The 3′ ends of most eukaryotic messenger RNAs are generated by internal cleavage and polyadenylation. In mammals, there is a strict dependence of both reactions on the sequence AAUAAA, which occurs upstream of polyadenylation [poly(A)] sites and which is recognized by CPSF. In contrast, cis-acting signals for yeast 3′-end generation are highly divergent from those of mammals, suggesting that trans-acting factors other than poly(A) polymerase would not be conserved. The essential yeast protein Brr5/Ysh1 shows sequence similarity to subunits of mammalian CPSF and is required for 3′-end processing in vivo and in vitro. These results demonstrate a structural and functional conservation of the yeast and mammalian 3′-end processing machineries despite a lack of conservation of the cis sequences.

The 3′ ends of most eukaryotic mRNAs are generated by a two-step mechanism in which endonucleolytic cleavage of the transcript is closely coupled with poly(A) addition (1). The virtually invariant sequence AAUAAA that lies 10 to 30 nucleotides upstream of mammalian poly(A) sites is essential to poly(A) site recognition and 3′-end formation (1). CPSF comprises three (2) to four (3) subunits and likely recognizes the AAUAAA sequence via the 160-kD

Department of Biochemistry and Biophysics, UCSF School of Medicine, San Francisco, CA 94143–0448. E-mail: guthrie@cgl.ucsf.edu

*Contributed equally to this work.
†To whom correspondence should be addressed.

subunit (1). In contrast, the sequences adjacent to poly(A) sites in yeast are highly divergent from those of mammals (4). Fractionation of yeast extracts has identified three fractions which, together with poly(A) polymerase, are necessary and sufficient to reconstitute cleavage and polyadenylation in vitro (5). Cleavage factor I (CFI) is required for both steps, cleavage factor II (CFII) is required only for cleavage, and polyadenylation factor I (PFI) is required solely for polyadenylation. Although a number of yeast 3′ processing factors have now been cloned and characterized (6, 7), none to date share sequence similarity with known CPSF subunits. In